European Radiology (2023) 33:5851–5855
https://doi.org/10.1007/s00330-023-09527-x

European Radiology
ESR EUROPEAN SOCIETY OF RADIOLOGY

EDITORIAL

MRI fat fraction imaging of nodal and bone metastases in prostate cancer

Cathy Qin[1] · Olivia Goldberg[1] · Geetanjali Kakar[1] · Simon Wan[2] · Athar Haroon[3] · Aishah Azam[4] · Sola Adeleke[5,6]

Received: 14 December 2022 / Revised: 14 December 2022 / Accepted: 5 February 2023 / Published online: 16 March 2023

Key Points

- *Characterisation and quantification of tissue fat on MRI can be used to provide information on disease processes.*
- *Fat in bone and lymph nodes up until recently have not been exploited for diagnostic purposes or response monitoring in prostate cancer.*
- *Fat imaging on MRI using Dixon/PDFF sequences has the potential to add clinical value in the future but prospective data is needed.*

Keywords Prostate cancer · Magnetic resonance imaging · Bone marrow · Lymphatic metastasis

Abbreviations

FF	Fat fraction
LN	Lymph node
mDIXON	Modified Dixon
Mp-MRI	Multi-parametric MRI
PCa	Prostate cancer
PDFF	Proton density fat fraction
PSMA PET-CT	Prostate specific membrane antigen PET-CT
sFF	Signal fat fraction
WB-MRI	Whole-body MRI

✉ Cathy Qin
cathy.qin2@nhs.net

1 Department of Radiology, Imperial College Healthcare NHS Trust, London, UK

2 Institute of Nuclear Medicine, University College London, London, UK

3 Department of Nuclear Medicine, Bart's Health NHS Trust, London, UK

4 Department of Radiology, Guy's and St Thomas' NHS Trust, London, UK

5 Department of Oncology, Guy's and St Thomas' NHS Trust, London, UK

6 School of Cancer and Pharmaceutical Sciences, Kings College London, London, UK

Introduction

Multi-parametric MRI (mp-MRI) plays a pivotal role in the prostate cancer (PCa) diagnostic pathway allowing for localisation, local staging and risk stratification [1]. Detection of lymph node (LN) and bony metastases is of utmost importance as this alters disease stage and management, and predicts biochemical recurrence following radiotherapy and overall survival [2]. The conventional imaging standard for detecting metastases utilises CT and bone scan, but increasingly prostate-specific membrane antigen PET/CT (PSMA PET-CT) is now used [3]. Whilst meta-analyses have demonstrated superiority of PSMA PET-CT in detecting metastatic disease compared to conventional imaging methods, it could be resource-intensive and not widely available [4].

Whole-body MRI (WB-MRI) has been gaining increasing traction as a non-ionising alternative, which may be more affordable and has potential comparative sensitivity to PSMA PET-CT in detecting bony metastases [5, 6]. Additionally, technological advances have potential to reduce scan time to under 1 h [7]. WB-MRI is also garnering interest as a plausible adjunct to mp-MRI to allow 'one-stop' comprehensive assessment of PCa [8]. With numerous MRI sequences at hand, new data is emerging on the most efficacious protocol to employ. This editorial focuses on the use of fat fraction (FF) imaging as a quantitative tool for assessing nodal and bony disease in PCa.

Dixon imaging and fat fraction sequences

Dixon imaging, which is routinely employed in WB-MRI, utilises the chemical shift property of protons to generate in-phase/opposed phase images. Then using mathematical reconstruction techniques, 'water-only' or 'fat-only' images are generated in a single acquisition [9]. This permits the derivation of fat content, expressed as 'signal fat fraction' (sFF), which is the signal generated by protons in fat as a fraction of total signal from fat and water protons within the voxel [10]. Proton density FF (PDFF) is equivalent to sFF in the absence of biophysical and technical factors that can confound the MR signal from fat and water [11]. It is thus considered a more accurate and reliable sequence [10, 11]. FF has been demonstrated to be useful in conditions such as hepatic steatosis and myeloma [12, 13]. Furthermore, previous studies have shown that using a modified Dixon protocol (mDixon) has similar diagnostic performance to conventional T1 fast spin echo for detecting nodal and bony metastases in PCa, whilst reducing WB-MRI acquisition time to < 20 min [7]. Depending on the parameters used, deriving sFF from this protocol may only add an extra minute to total scan time [14].

Detecting nodal and bone metastases

Nodal disease is determined primarily by size on CT and MRI where a threshold of >1 cm in short axis dimension indicates metastatic involvement [15]. However, it has been shown that around 10–35% of 'normal' size LNs harbour microscopic metastases on histology [16, 17]. Moreover, false positives can occur in the context of reactive hyperplasia and granulomatous infiltration [18]. This may produce inaccuracies in nodal staging by conventional CT and/or MRI [19].

PCa predominantly causes sclerotic bony lesions [20]. DWI is widely used in assessing bony disease but can be prone to false positives in the context of traumatic oedema, degenerative disease, infection, infarction and hypercellular red marrow deposits, resulting in reduced sensitivity [21]. DWI is also vulnerable to motion and susceptibility artefact which can limit its interpretation [22].

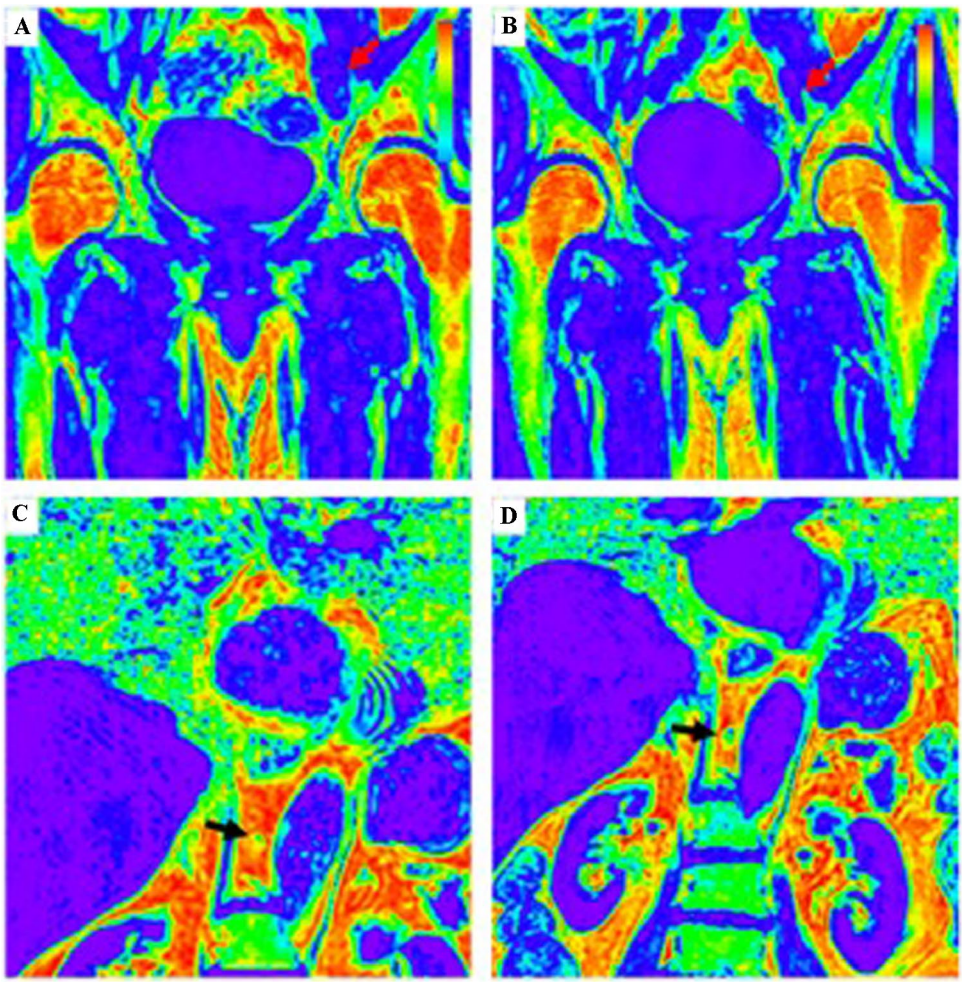

Fig. 1 Fat fraction changes in nodal lesions following systemic therapy for responding and non-responding lesions. Red areas on the colour scale indicates fat fraction of 100%, while blue areas indicate little or no fat content. Fat fraction map changes in a responding large left external iliac node (red arrow) pre (**A**) and post-treatment (**B**) shows little to no fat content at baseline. A poorly responsive paraaortic node (black arrows) shows high fat content at baseline (**C**) and loss of fat at 1 year (**D**) following systemic therapy. (Included with permission from Adeleke 2020) [25]

Recent evidence for fat fraction imaging

Nodal metastases

Nodal disease assessment using sFF has been demonstrated in several small-scale studies. O'Callaghan et al analysed mDIXON MRI data in 5 men with PCa and PET-proven nodal disease and found that sFF was significantly lower in those nodes with ^{18}F-choline PET-positivity compared to PET-negative nodes despite no significant difference in LN size [23]. Similar findings were reported in a retrospective analysis of 43 nodes in 11 patients: mean sFF was significantly lower in ^{18}F-choline PET-positive nodes, but there was no statistical difference in size, T2 signal or ADC demonstrated between positive and negative nodes [24]. A larger study assessing 131 nodes in 40 patients with radio-recurrent disease highlighted the discriminatory ability of sFF as a marker of nodal disease status and exhibited excellent accuracy (ROC-AUC 0.86) [17]. Furthermore, in the same study, across 28 nodes in 13 patients who received androgen deprivation therapy, baseline median sFF was significantly lower across treatment responders than non-responders (Fig. 1). This highlights the potential of sFF to be a predictor of treatment response in the radio-recurrent cohort [17].

Bone metastases

sFF can also assess derangements in marrow fat, which has been shown to correlate with histological and molecular analyses [26]. A pilot study on castration-resistant PCa found that sFF was significantly lower in bony metastases compared to normal bone; median sFF was 14% in positive biopsies compared to 71% in normal biopsies ($p < 0.05$) [27]. sFF has also been shown to be a predictor of response in bony lesions. In a study involving 17 patients with radio-recurrent disease (22 bony lesions) who received systemic therapy, baseline median sFF was significantly lower in lesions that responded compared to non-responders [25] (Fig. 2).

Similar findings have been reported using PDFF. Schmeel et al prospectively evaluated 66 patients (11 patients had PCa) who were referred for MRI spine and found PDFF was significantly lower in malignant spine

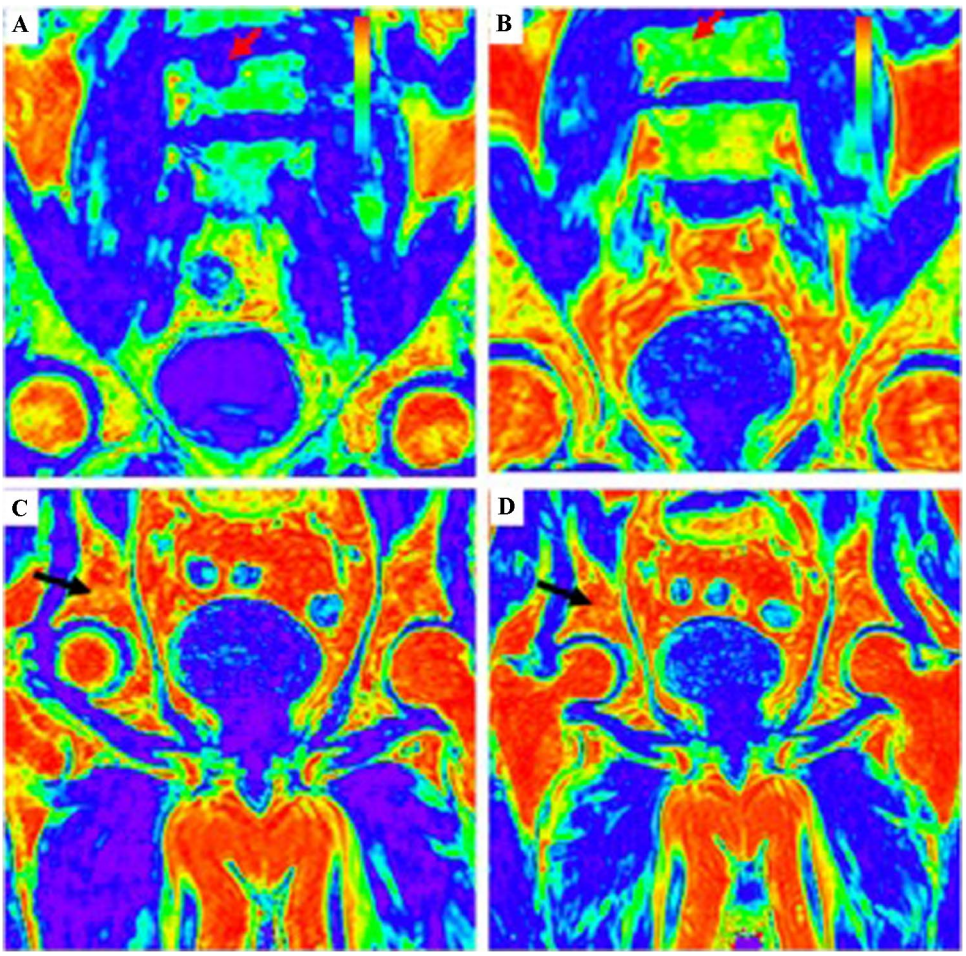

Fig. 2 Fat fraction changes in bone lesions following systemic therapy for responding and non-responding lesions. Red coloured areas on the scale indicates fat fraction of 100% whilst blue indicates little or no fat content. Changes in fat fraction maps pre-treatment (**A**) and post-treatment (**B**) for a responding lesion in the L4 vertebral body (red arrow). A non-responding lesion in the right pelvis (black arrow) at baseline (**C**), which has not changed at 1 year (**D**) following systemic therapy. (Included with permission from Adeleke 2020) [25]

lesions compared to benign lesions such as osteoporosis, end-plate degeneration and haemangiomas. Furthermore, ROC analysis of PDFF cutoff values found a PDFF of 6.4% was optimal in differentiating between malignant and benign causes with an AUC of 0.97 [14]. A similar cutoff was reported by Yoo et al [28]. This may help to prevent unnecessary downstream invasive investigations such as bone biopsies.

The diagnostic accuracy of sFF compared to DWI has also been directly compared. Donners et al retrospectively evaluated 42 malignant (12 of whom had PCa) and 27 osteoporotic vertebral fractures in 38 patients. Whilst both sFF and ADC were significantly lower in pathological fractures compared to non-malignant fractures, the AUC value of sFF was significantly higher than that of ADC [29]. Kwack et al reported similar findings when assessing the diagnostic performance of PDFF versus ADC in differentiating between benign and malignant causes of vertebral bone marrow lesions and found PDFF had significantly higher diagnostic accuracy [30].

Conclusion

Recent evidence has highlighted the feasibility of sFF as a rapid sequence which can detect malignant nodal and bone lesions. sFF has also been shown to have comparable or even superior diagnostic accuracy to ADC when evaluating benign versus malignant bone marrow lesions. sFF could compliment DWI and could potentially be incorporated into the routine mp-MRI protocol and/or routinely derived in WB-MRI protocol in the PCa imaging pathway. Further large-scale, prospective studies involving different PCa cohorts are required to corroborate these findings and to compare FF to other reference standards.

Funding The authors state that this work has not received any funding.

Declarations

Guarantor The scientific guarantor of this publication is Dr Sola Adeleke.

Conflict of interest The authors of this manuscript declare no relationships with any companies whose products or services may be related to the subject matter of the article.

Statistics and biometry No complex statistical methods were necessary for this paper.

Informed consent Not applicable.

Ethical approval Not applicable.

Methodology
• Editorial

References

1. Turkbey B, Brown AM, Sankineni S, Wood BJ, Pinto PA, Choyke PL (2016) Multiparametric prostate magnetic resonance imaging in the evaluation of prostate cancer. CA Cancer J Clin 66(4):326–336
2. Turpin A, Girard E, Baillet C et al (2020) Imaging for Metastasis in Prostate Cancer: A Review of the Literature. Front Oncol 10:55. https://doi.org/10.3389/fonc.2020.00055
3. Ghafoor S, Burger IA, Vargas AH (2019) Multimodality Imaging of Prostate Cancer. J Nucl Med 60(10):1350–1358
4. Wang Y, Galante JR, Haroon A et al (2022) The future of PSMA PET and WB MRI as next-generation imaging tools in prostate cancer. Nat Rev Urol 19(8):475–493
5. Van Damme J, Tombal B, Collette L et al (2021) Comparison of (68)Ga-Prostate Specific Membrane Antigen (PSMA) Positron Emission Tomography Computed Tomography (PET-CT) and Whole-Body Magnetic Resonance Imaging (WB-MRI) with Diffusion Sequences (DWI) in the Staging of Advanced Prostate Cancer. Cancers (Basel) 13(21):5286. https://doi.org/10.3390/cancers13215286
6. Zhan Y, Zhang G, Li M, Zhou X (2021) Whole-Body MRI vs. PET/CT for the detection of bone metastases in patients with prostate cancer: a systematic review and meta-analysis. Front Oncol 11:633833. https://doi.org/10.3389/fonc.2021.633833
7. Lecouvet FE, Pasoglou V, Van Nieuwenhove S et al (2020) Shortening the acquisition time of whole-body MRI: 3D T1 gradient echo Dixon vs fast spin echo for metastatic screening in prostate cancer. Eur Radiol 30(6):3083–3093
8. Pasoglou V, Michoux N, Tombal B, Lecouvet F (2016) Optimising TNM Staging of Patients with Prostate Cancer Using WB-MRI. J Belg Soc Radiol 100(1):101
9. Ma J (2008) Dixon techniques for water and fat imaging. J Magn Reson Imaging 28(3):543–558
10. Bray TJ, Chouhan MD, Punwani S, Bainbridge A, Hall-Craggs MA (2018) Fat fraction mapping using magnetic resonance imaging: insight into pathophysiology. Br J Radiol 91(1089):20170344
11. Reeder SB, Hu HH, Sirlin CB (2012) Proton density fat-fraction: a standardized MR-based biomarker of tissue fat concentration. J Magn Reson Imaging 36(5):1011–1014
12. Ajmera V, Park CC, Caussy C et al (2018) Magnetic Resonance Imaging Proton Density Fat Fraction Associates With Progression of Fibrosis in Patients With Nonalcoholic Fatty Liver Disease. Gastroenterology. 155(2):307–10.e2
13. Latifoltojar A, Hall-Craggs M, Rabin N et al (2017) Whole body magnetic resonance imaging in newly diagnosed multiple myeloma: early changes in lesional signal fat fraction predict disease response. Br J Haematol 176(2):222–233
14. Schmeel FC, Luetkens JA, Wagenhäuser PJ et al (2018) Proton density fat fraction (PDFF) MRI for differentiation of benign and malignant vertebral lesions. Eur Radiol 28(6):2397–2405
15. Eisenhauer EA, Therasse P, Bogaerts J et al (2009) New response evaluation criteria in solid tumours: revised RECIST guideline (version 1.1). Eur J Cancer 45(2):228–247
16. Gross BH, Glazer GM, Orringer MB, Spizarny DL, Flint A (1988) Bronchogenic carcinoma metastatic to normal-sized lymph nodes: frequency and significance. Radiology. 166(1 Pt 1):71–74
17. Adeleke S (2019) Fat fraction provides classification and treatment response assessment of metastatic lymph nodes for patients with radio-recurrent prostate cancer. Presented at: ISMRM 27th Annual Meeting and Exhibition, Montreal
18. Zarzour JG, Galgano S, McConathy J, Thomas JV, Rais-Bahrami S (2017) Lymph node imaging in initial staging of prostate cancer: An overview and update. World J Radiol 9(10):389–399

19. Adeleke S, Latifoltojar A, Sidhu H et al (2019) Localising occult prostate cancer metastasis with advanced imaging techniques (LOCATE trial): a prospective cohort, observational diagnostic accuracy trial investigating whole–body magnetic resonance imaging in radio-recurrent prostate cancer. BMC Med Imaging 19(1):90
20. Messiou C, Cook G, deSouza NM (2009) Imaging metastatic bone disease from carcinoma of the prostate. Br J Cancer 101(8):1225–1232
21. Padhani AR, Gogbashian A (2011) Bony metastases: assessing response to therapy with whole-body diffusion MRI. Cancer Imaging 11 Spec No A(1a):S129-45
22. Raya JG, Dietrich O, Reiser MF, Baur-Melnyk A (2005) Techniques for diffusion-weighted imaging of bone marrow. Eur J Radiol 55(1):64–73
23. O'Callaghan J, Johnston E, Latifoltojar A et al (2017) Improved lymph node staging using MRI mDixon fat fraction measurements in patients with intermediate and high-risk prostate cancer. ISMRM 25th Annual Meeting & Exhibition Conference
24. Appayya MB, O'Callaghan J, Latifoltojar A et al (2018) Quantitative mDixon Fat Fraction can differentiate metastatic nodes from benign nodes in prostate cancer patients. Proc Int Soc Mag Reson Med 26:0721
25. Adeleke S (2020) Qualitative and quantitative whole-body MRI assessment of metastatic disease in patients with radio-recurrent prostate cancer [Dissertation on the internet]. United Kingdom: University College London. https://discovery.ucl.ac.uk/id/eprint/10119042
26. Perez-Lopez R, Nava Rodrigues D, Figueiredo I et al (2018) Multiparametric Magnetic Resonance Imaging of Prostate Cancer Bone Disease: Correlation With Bone Biopsy Histological and Molecular Features. Invest Radiol 53(2):96–102
27. Kossov F, van Steenbergen T, Smits M et al (2019) Detection and differentiation of bone metastases in castration resistant prostate cancer (CRPC) patients using 68Ga-PSMA-PET/CT and MR molecular imaging compared to bone biopsy histology as a gold standard. A pilot study: Part I. European Congress of Radiology-ECR
28. Yoo HJ, Hong SH, Kim DH et al (2017) Measurement of fat content in vertebral marrow using a modified dixon sequence to differentiate benign from malignant processes. J Magn Reson Imaging 45(5):1534–1544
29. Donners R, Obmann MM, Boll D, Gutzeit A, Harder D (2020) Dixon or DWI – Comparing the utility of fat fraction and apparent diffusion coefficient to distinguish between malignant and acute osteoporotic vertebral fractures. Eur J Radiol 132:109342
30. Kwack KS, Lee HD, Jeon SW, Lee HY, Park S (2020) Comparison of proton density fat fraction, simultaneous R2*, and apparent diffusion coefficient for assessment of focal vertebral bone marrow lesions. Clin Radiol 75(2):123–130